

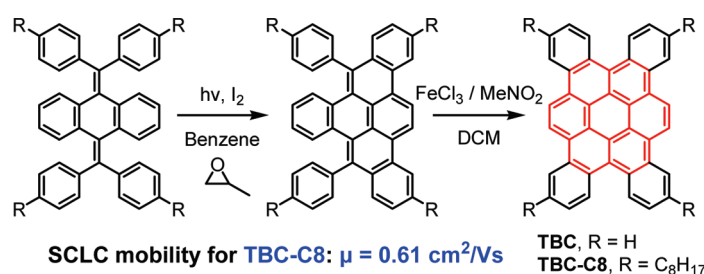
Synthesis, Self-Assembly, and Charge Transporting Property of Contorted Tetrabenzocoronenes

Xiaojie Zhang,[†] Xiaoxia Jiang,^{*,‡} Kai Zhang,[†] Lu Mao,[†] Jing Luo,[†] Chunyan Chi,[†] Hardy Sze On Chan,[†] and Jishan Wu^{*,†}

[†]Department of Chemistry, National University of Singapore, 3 Science Drive 3, Singapore, 117543, and
[‡]Department of Polymer Science and Engineering, Zhejiang University, Hangzhou, People's Republic of China, 310027

chmwuj@nus.edu.sg; plyjxx@zju.edu.cn

Received August 30, 2010



A facile route has been developed for the preparation of a new family of contorted 1,2,3,4,7,8,9,10-tetrabenzocoronenes (TBCs). A two-step cyclization reaction, i.e., oxidative photocyclization followed by FeCl₃-mediated intramolecular cyclodehydrogenation, was carried out on the olefin precursors to obtain the final TBC compounds. These new TBC molecules have contorted conformation due to steric overcrowding as disclosed by single-crystal crystallographic analysis. Nevertheless, they showed extended π -conjugation compared with coronene and exhibited strong aggregation in solution. The thermal behavior and self-assembly of TBC-C8 in solid were studied by a combination of thermogravimetric analysis (TGA), differential scanning calorimetry (DSC), powder X-ray diffraction (XRD), scanning electron microscope (SEM), and transmission electron microscope (TEM). Compound TBC-C8 showed very good thermal and photostability and exhibited long-range ordered π -stacking in the bulk state. Moreover, uniform nanofibers with tens of micrometer length are formed in the drop-casted thin films. TBC-C8 also possesses a desirable HOMO energy level (-5.10 eV), which allows efficient charge injection from electrodes such as gold electrode. The charge carrier mobilities were determined by using the space-charge limited-current (SCLC) technique and high average hole mobility of $0.61 \text{ cm}^2 \text{ V}^{-1} \text{ s}^{-1}$ was obtained for TBC-C8.

Introduction

Disk-like polycyclic aromatic hydrocarbons (PAHs) with columnar superstructures formed by π -stacking¹ have been shown to exhibit high one-dimensional charge-carrier mobilities along the stacking axis and thus they are potential

semiconductors for organic field-effect transistors (FETs),² solar cells,³ and molecular electronic devices.⁴ The planarity, core size, and electron distribution of a PAH are supposed to

(1) (a) Clar, E. *Polycyclic Hydrocarbons*; Academic Press: New York, 1964; Vols. 1 and 2. (b) Ronald, G. H.; *Polycyclic Aromatic Hydrocarbons*; Wiley, VCH: New York, 1997. (c) Wu, J.; Pisula, W.; Müllen, K. *Chem. Rev.* **2007**, *107*, 718–747. (d) Laschat, S.; Baro, A.; Steinke, N.; Giesselmann, F.; Hagele, C.; Scalia, G.; Judele, R.; Kapatsina, E.; Sauer, S.; Schreivogel, A.; Tosoni, M. *Angew. Chem., Int. Ed.* **2007**, *46*, 4832–4887. (e) Feng, X.; Liu, M.; Pisula, W.; Takase, M.; Li, J.; Müllen, K. *Adv. Mater.* **2008**, *20*, 2684–2689.

(2) (a) Bendikov, M.; Wudl, F. *Chem. Rev.* **2004**, *104*, 4891–4945. (b) Zhang, Y.; Petta, J. R.; Ambily, S.; Shen, Y.; Ralph, D. C.; Malliaras, G. G. *Adv. Mater.* **2003**, *15*, 1632–1635. (c) Butko, V. Y.; Chi, X.; Lang, D. V.; Ramirez, A. P. *Appl. Phys. Lett.* **2003**, *83*, 4773–4775. (d) Jurchescu, O. D.; Popinciuc, M.; van Wees, J.; Palstra, B.; Thomas, T. M. *Adv. Mater.* **2007**, *19*, 688–692. (e) Anthony, J. E. *Angew. Chem., Int. Ed.* **2008**, *47*, 452–483.

(3) (a) Li, J.; Kastler, M.; Pisula, W.; Robertson, J. W. F.; Wasserfallen, D.; Grimsdale, A. C.; Wu, J.; Müllen, K. *Adv. Funct. Mater.* **2007**, *17*, 2528–2533. (b) Schmidt-Mende, L.; Fechtenkötter, A.; Müllen, K.; MacKenzie, J. D. *Science* **2001**, *293*, 1119–1122.

(4) Jäckel, F.; Watson, M. D.; Müllen, K.; Rabe, J. P. *Phys. Rev. Lett.* **2004**, *92*, 188303.

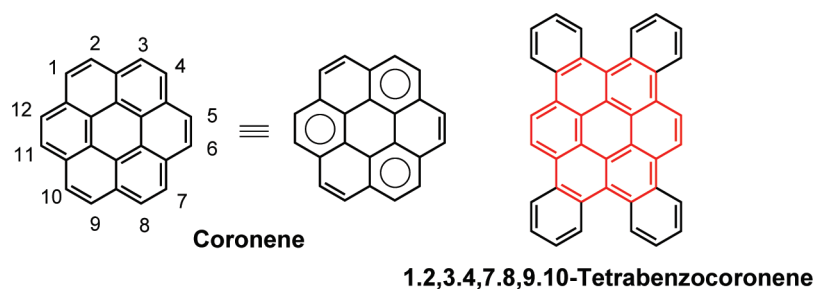


FIGURE 1. Structures of coronene and 1,2,3,4,7,8,9,10-tetrabenzocoronene.

play key roles on their self-assembling and charge transporting properties.⁵

Among many benzenoid PAHs, coronene (Figure 1) represents the smallest homologue of benzene with 6-fold symmetry, giving it a unique electronic structure due to the perfect delocalization of aromaticity between the six outer rings.⁶ According to Clar's aromatic sextet rule, three full benzenoid aromatic sextet rings can be drawn (Figure 1) for coronene and this results in a high chemical stability compared to other linear and meta-annulated aromatics such as acenes and phenes.^{1a} In the crystalline state, coronene forms a columnar structure with π -stacking with an exceptionally short distance of 3.43 Å between the aromatic planes.⁷ Thus the overlap of π orbitals between neighboring planes is large and charge carriers can travel easily along the columns.⁸ Chemical modifications of coronene have been carried out to tune its electronic properties and self-assembly. For example, flexible chain-substituted coronenes showed highly ordered columnar liquid-crystalline phases over wide temperature ranges.^{6a} At the same time, either electron-donating or electron-withdrawing groups can be introduced onto the coronene core to tune its electronic structure.^{6b,9} Besides substitution, fusion of additional benzenoid rings onto the coronene core is an alternative way to generate new disk-like PAH molecules with intriguing properties. For example, the *peri*-fused hexa-*peri*-hexabenzocoronene derivatives reported by Müllen et al. have shown excellent chemical and thermal stability, highly ordered self-assembly in the bulk state, and high one-dimensional charge carrier mobility,

which qualified them as useful semiconductors for high-performance electronic devices.^{1c,10,11} The *cata*-fused hexa-*cata*-hexabenzocoronene reported by Nuckolls et al. also exhibited very interesting self-assembling and charge transporting properties.¹² In this work, we are particularly interested in a new coronene-based hydrocarbon, the 1,2,3,4,7,8,9,10-tetrabenzocoronene (**TBC**, Figure 1), which is supposed to show unique structural, self-assembling, and charge transporting properties. This framework is expected to be contorted due to steric overcrowding between the neighboring outer benzenoid rings. The molecule does not possess an all-benzenoid character and thus its electronic structure should be different from that of the all-benzenoid hexa-*peri*-hexabenzocoronene and coronene itself. Moreover, whether this type of contorted molecules can self-assemble into ordered columnar structure is also of interest when considering their potential applications in electronic devices.

Synthesis of coronene and its derivatives is not an easy task and the methods reported earlier usually suffered from lengthy procedures and low yields.¹³ In recent years milder methods giving higher yields and higher selectivity have been explored,¹⁴ but the lack of a convenient and efficient synthesis of coronenes still impedes their practical applications in materials science. Synthesis of benzenoid ring fused coronenes such as **TBCs** is also challenging. In this paper, we report the efficient synthesis of the contorted tetrabenzocoronenes (**TBC** and the alkylated **TBC-C8**, Scheme 1) by using high-yielding stepwise photocyclization followed by Scholl-type oxidative cyclodehydrogenation reaction of appropriate aryl-substituted/fused olefin precursors, which can be prepared by the Barton–Kellogg olefination reaction¹⁵ in high yields. Our approach provided a rapid and large-quantity synthesis of **TBC**-based materials. The photophysical properties of **TBCs** were studied by UV–vis absorption and fluorescence spectroscopy and their electrochemical properties were investigated by cyclic voltammetry (CV). Their self-assembly in solution was investigated by varied-temperature

(5) (a) Goddard, R.; Haenel, M. W.; Herndon, W. C.; Krieger, C.; Zander, M. *J. Am. Chem. Soc.* **1995**, *117*, 30–41. (b) Kastler, M.; Schmidt, J.; Pisula, W.; Sebastiani, D.; Müllen, K. *J. Am. Chem. Soc.* **2006**, *128*, 9526–9534.

(6) (a) Alibert-Fouet, S.; Seguy, I.; Bobo, J.; Destruel, P.; Bock, H. *Chem.—Eur. J.* **2007**, *13*, 1746–1753. (b) Rieger, R.; Kastler, M.; Enkelmann, V.; Müllen, K. *Chem.—Eur. J.* **2008**, *14*, 6322–6325. (c) Steiner, E.; Fowler, P. W.; Jennekens, L. W. *Angew. Chem., Int. Ed.* **2001**, *40*, 362–366.

(7) (a) Matsui, A. H.; Mizuno, K.-I. *J. Phys. D: Appl. Phys.* **1993**, *26*, B242–244. (b) Robertson, J. M.; White, J. G. *J. Chem. Soc.* **1945**, 607–616.

(8) (a) Adam, D.; Schuhmacher, P.; Simmerer, J.; Haeussling, L.; Siemsmeyer, K.; Etzbach, K. H.; Ringsdorf, H.; Haarer, D. *Nature* **1994**, *371*, 141–143. (b) van de Craats, A. M.; Warman, J. M.; Fechtenkötter, A.; Brand, J. D.; Harbison, M. A.; Müllen, K. *Adv. Mater.* **1999**, *11*, 1469–1472. (c) Warman, J. M.; de Haas, M. P.; Dicker, G.; Grozema, F. C.; Piris, J.; Debye, M. G. *Chem. Mater.* **2004**, *16*, 4600–4609.

(9) (a) Rohr, U.; Schlichting, P.; Böhm, A.; Gross, M.; Meerholz, K.; Bräuchle, C.; Müllen, K. *Angew. Chem., Int. Ed.* **1998**, *37*, 1434–1437. (b) Rohr, U.; Kohl, C.; Müllen, K.; van de Craats, A.; Warman, J. *J. Mater. Chem.* **2001**, *11*, 1789–1799. (c) Jia, H.; Liu, S.; Sanguinet, L.; Levillain, E.; Decurtins, S. *J. Org. Chem.* **2009**, *74*, 5727–5729. (d) Rao, K. V.; George, S. J. *Org. Lett.* **2010**, *12*, 2656–2659.

(10) (a) Watson, M. D.; Fechtenkötter, A.; Müllen, K. *Chem. Rev.* **2001**, *101*, 1267–1300. (b) Simpson, C. D.; Wu, J.; Watson, M. D.; Müllen, K. *J. Mater. Chem.* **2004**, *14*, 494–504.

(11) (a) Sakurai, H.; Daiko, T.; Hirao, T. *Science* **2003**, *301*, 1878. (b) Hill, J. P.; Jin, W. S.; Kosaka, A.; Fukushima, T.; Ichihara, H.; Shimomura, T.; Ito, K.; Hashizume, T.; Ishii, N.; Aida, T. *Science* **2004**, *304*, 1481–1483.

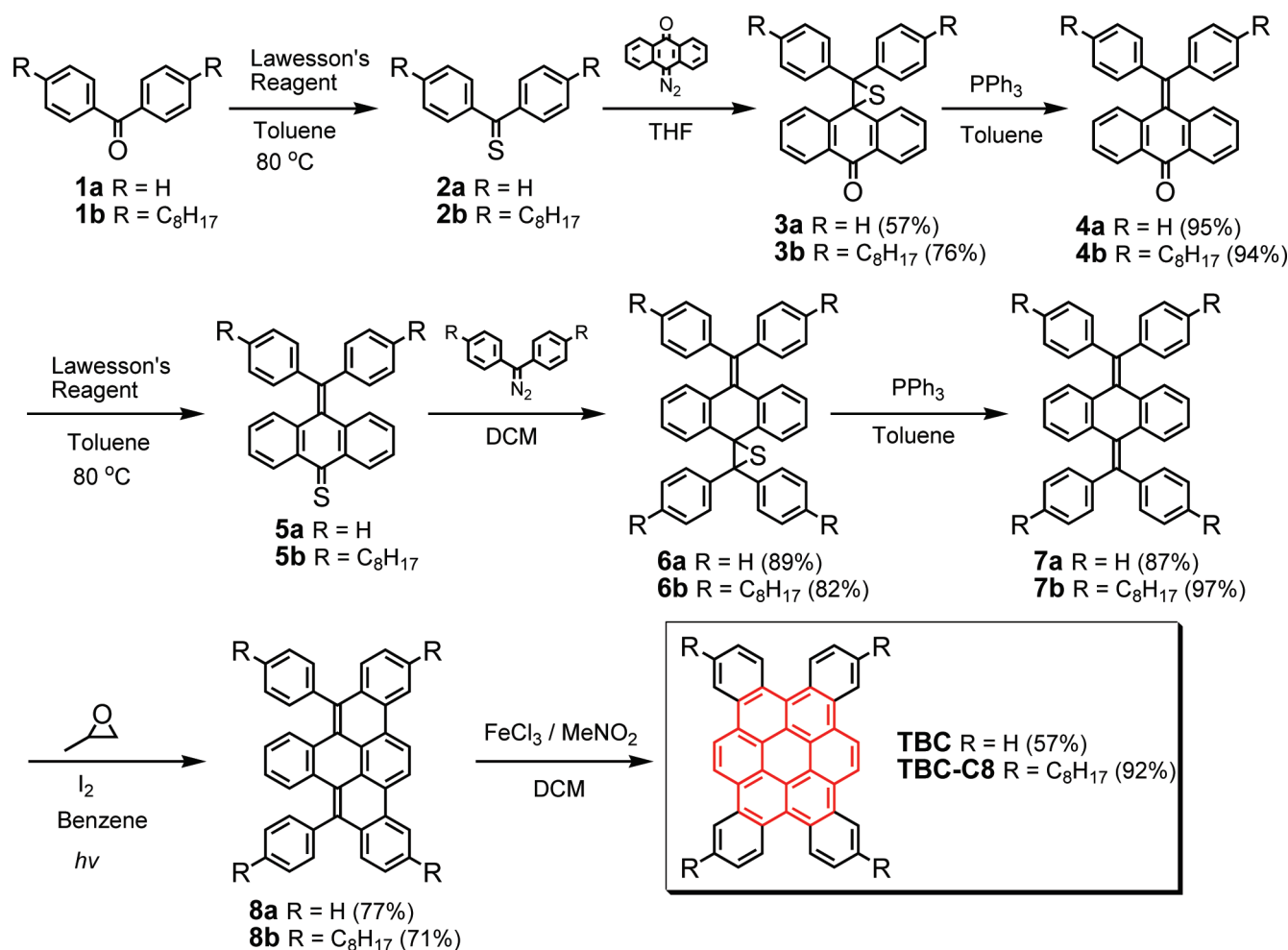
(12) (a) Xiao, S.; Myers, M.; Miao, Q.; Sanaur, S.; Pang, K.; Steigerwald, M. L.; Nuckolls, C. *Angew. Chem., Int. Ed.* **2005**, *44*, 7390–7394. (b) Xiao, S.; Tang, J.; Beetz, T.; Guo, X.; Tremblay, N.; Siegrist, T.; Zhu, Y.; Steigerwald, M.; Nuckolls, C. *J. Am. Chem. Soc.* **2006**, *128*, 10700–10701. (c) Plunkett, K. N.; Godula, K.; Nuckolls, C.; Tremblay, N.; Whalley, A. C.; Xiao, S. *Org. Lett.* **2009**, *11*, 2225–2228.

(13) (a) Scholl, R.; Meyer, K. *Ber. Dtsch. Chem. Ges.* **1932**, *65*, 902–915. (b) Newman, M. *J. Am. Chem. Soc.* **1940**, *62*, 1683–1687. (c) Clar, E.; Zander, M. *J. Chem. Soc.* **1957**, 4616–4619.

(14) (a) Van Dijk, J. T. M.; Hartwijk, A.; Bleeker, A. C.; Lugtenburg, J.; Cornelusse, J. *J. Org. Chem.* **1996**, *61*, 1136–1139. (b) Shen, H.; Tang, J.; Chang, H.; Yang, C.; Liu, R. *J. Org. Chem.* **2005**, *70*, 10113–10116.

(15) (a) Barton, D. H. R.; Willis, B. J. *J. Chem. Soc. D* **1970**, 1225–1226. (b) Kellogg, R. M.; Wassenaar, S. *Tetrahedron Lett.* **1970**, *11*, 1987–1990. (c) Feringa, B. L. *Acc. Chem. Res.* **2001**, *34*, 504–513.

SCHEME 1. Synthetic Route Toward Compounds TBC and TBC-C8



(VT) NMR spectroscopy and the morphology of drop-cast films from solution was probed by scanning electron microscope (SEM) and transmission electron microscope (TEM). Their thermal behavior and molecular packing in the solid state were also studied by thermogravimetric analysis (TGA), differential scanning calorimetry (DSC), powder X-ray diffraction (XRD), and single-crystal crystallographic analysis. Their charge transporting property in thin films was measured by space-charge limited-current (SCLC) technique. All these studies are necessary for their potential applications in electronic devices such as OLEDs, OFETs, and solar cells.

Results and Discussion

Synthesis of TBC and TBC-C8. Scheme 1 outlines the synthesis of **TBC** and **TBC-C8**. The strategy is to first synthesize the olefin precursors such as **7a** and **7b** and this is followed by intramolecular cyclization reactions to give the target tetrabenzocoronene compounds. The Barton–Kellogg reaction is a powerful tool for preparing tetra-substituted alkenes by reaction of a thioketone with a diazomethane followed by reduction with triphenylphosphine.¹⁵ Thus, this reaction was used to prepare the precursors **7a** and **7b**. Our synthesis began with benzophenone (**1a**) and 4,4'-dioctylbenzophenone (**1b**, see the synthesis in the Supporting Information), which were heated at 80 °C in dry toluene

with Lawesson's reagent to give the corresponding thioketones **2a** and **2b**. Unfortunately, we were unable to isolate the thioketones in pure form due to the poor stability of **2a** and **2b**, and the crude product was therefore used to directly react with 1.2 mol equiv of the 10-diazoanthrone¹⁶ to give the thioepoxides **3a** and **3b** in 57% and 76% yield, respectively. Reduction of the thioepoxide functionality with triphenylphosphine produced the desired ketones **4a** and **4b** in 95% and 94% yield, respectively. Similar reactions were used in the synthesis of olefins **7a** and **7b**. The thioquinones **5a** and **5b** were prepared from corresponding ketones **4a** and **4b** via reaction with Lawesson's reagent followed by the Barton–Kellogg reaction with diphenyldiazomethane derived from corresponding hydrazones^{12a} to afford the thioepoxides **6a** and **6b** in 89% and 82% yield. The resulting compounds **6a** and **6b** were then treated with triphenylphosphine in refluxing toluene to give the desired olefins **7a** and **7b** in 87% and 97% yield, respectively.

The key step for the synthesis of **TBC** and **TBC-C8** was the intramolecular cyclodehydrogenation reactions of **7a** and **7b**. We first attempted to use a Katz-modified Mallory photocyclization method to prepare the **TBC** compounds.¹⁷ The

(16) Raasch, M. S. *J. Org. Chem.* **1979**, *44*, 632–633.

(17) Liu, L.; Yang, B.; Katz, T.; Poindexter, M. K. *J. Org. Chem.* **1991**, *56*, 3769–3775.

reaction was conducted by irradiation of the benzene solution of **7a** or **7b** with a 450 W medium-pressure mercury vapor lamp in the presence of I_2 and propylene oxide and followed by purification by column chromatography. Interestingly, the partially cyclized compounds **8a** and **8b** were obtained in 77% and 71% yield, respectively. Extension of the reaction time did not provide any fully cyclized product. To further understand the possible reasons for this unusual reaction, a single crystal of **8a** suitable for crystallographic analysis was successfully grown by slow diffusion of methanol to the chloroform solution and the single-crystal structure is presented in Figure 2. It is clear that only the cis-fused compound **8a** was formed with formation of two new C–C bonds. It is worth noting that the C7–C8 and C15–C16 bonds are as long as 1.405 Å (highlighted with a red arrow in Figure 2), which is close to the average carbon–carbon bond length in an aromatic benzene ring (1.38–1.40 Å). This bond length is significantly longer than that of an isolated carbon–carbon double bond (1.35 Å), indicating that after cyclization reaction the C7–C8 and C15–C16 bonds exhibit a typical delocalized double bond character for an aromatic system instead of an isolated double bond feature. Since the photocyclization follows a mechanism similar to the photocyclization

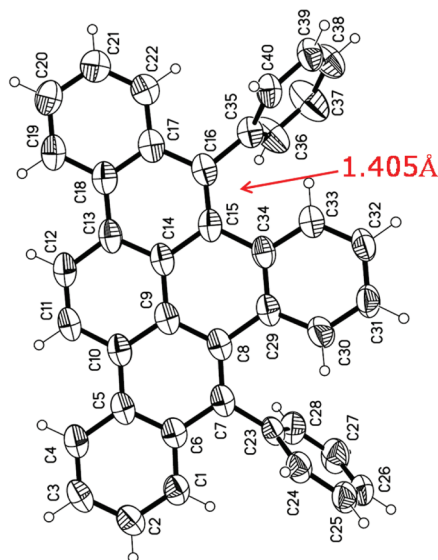


FIGURE 2. Single-crystal structure of compound **8a**.

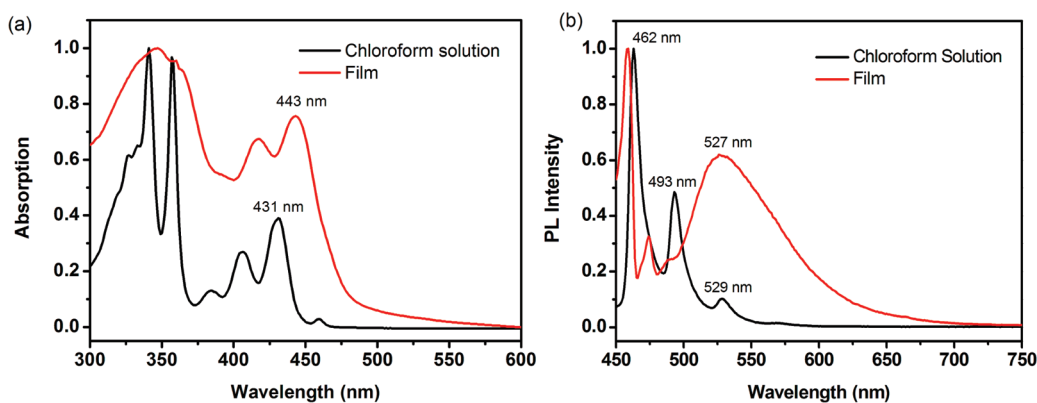


FIGURE 3. (a) Normalized UV–vis absorption spectra of **TBC-C8** in $CHCl_3$ and in thin film; (b) normalized photoluminescence spectra of **TBC-C8** in $CHCl_3$ and in thin film.

of stilbene-type precursors, it is understandable that the photocyclization stopped at the partially cyclized intermediates such as **8a** and **8b** because there are no more stilbene structures in these intermediates. Bond length measurements also disclosed that the other fused or unfused rings all showed typical aromatic benzenoid character, thus we expect that further cyclization by a Scholl-type reaction is possible. In the next step oxidative cyclodehydrogenation was conducted by treating **8a** and **8b** with ferric chloride in nitromethane and dichloromethane (DCM), a typical procedure to convert appropriate branched oligophenylene precursors to fused disk-like PAHs,^{1c} and the target compounds **TBC** and **TBC-C8** were obtained in 57% and 92% yield, respectively. Compound **TBC** was obtained as a yellow powder after repeated washing with methanol, hexane, and chloroform and it was insoluble in common organic solvents. The tetraoctyl-substituted compound **TBC-C8** is readily dissolved in common organic solvents, such as hexane, DCM, chloroform, toluene, and THF, which allows us to purify it by column chromatography. Both compounds are also very stable under ambient conditions. For example, the air-saturated solution of **TBC-C8** in toluene was submitted to irradiation by UV lamp (4 W) and there was no change on the absorption spectrum even after irradiation for 1 week. The structures of these new compounds were identified by 1H NMR and ^{13}C NMR spectroscopy, elemental analysis, and mass spectroscopy. Furthermore, we also attempted the synthesis of **TBC** directly from **7a** by using $FeCl_3$ /nitromethane/DCM condition and the starting material decomposed and gave some uncharacterizable byproducts. Thus, it is essential to conduct such a two-step cyclization process to make the target compounds. Such a method is also scalable and represents an efficient synthetic approach toward tetrabenzocoronenes.

Optical and Electrochemical Properties of TBC-C8 and Its Self-Assembly in Solution. The UV–vis absorption spectra of **TBC-C8** in chloroform and thin film are shown in Figure 3a. The **TBC-C8** shows well-resolved absorption bands between 300 and 500 nm with a long wavelength absorption maximum at 431 nm (*p* band, $\log \epsilon = 4.60$; ϵ is the molar extinction coefficient, in $M^{-1} cm^{-1}$). A weak α band at 462 nm ($\log \epsilon = 3.52$) was also observed. For comparison, the absorption spectrum of coronene shows a *p* band at 342 nm ($\log \epsilon = 4.85$) and a very weak α band at 428 nm ($\log \epsilon = 2.15$) in benzene.¹³ This suggests that fusion of an additional four benzenoid rings to the coronene core leads to an extended π -conjugation

and red-shift of the absorption spectrum. The absorption spectrum in drop-casted film exhibits a considerable bathochromic (12 nm) shift and spectral broadening, indicating that the chromophores have a strong tendency to aggregate in the solid state. Photoluminescence spectra of the **TBC-C8** in chloroform and in thin film are shown in Figure 3b. Three distinct emission bands with maxima at 462, 493, and 529 nm were observed in solution. The thin film photoluminescence spectrum of the **TBC-C8** shows a broad emission band centered at 527 nm, together with a long tail at the low-energy side, again, implying the existence of chromophore aggregation in the solid state.

The electrochemical property of compound **TBC-C8** was studied by cyclic voltammetry and differential pulse voltammetry (DPV) in DCM at room temperature. As shown in Figure 4, four quasireversible oxidation waves with half-wave potentials at 0.84, 0.96, 1.28, and 1.42 V (vs Ag/AgCl) were observed, indicating that the **TBC-C8** can be oxidized into charged states which are stabilized by the largely delocalized π -system. A HOMO energy level of 5.10 eV was estimated for **TBC-C8** based on the onset potential (E_{ox}^1) of the first oxidation waves.¹⁸ Interestingly, the HOMO energy level of the expanded core molecule **TBC-C8** matches well with the work function of the gold electrode ($w \approx 5.1$ eV),¹⁹ which is a commonly used electrode in FETs. This character is supposed to ensure efficient hole injection during the operation of a FET device.

As mentioned above, the **TBC-C8** showed an obvious red-shift of its absorption and emission spectra upon going from solution to solid state, suggesting that the molecules actually have strong intermolecular interactions. To further understand its self-assembly in solution, temperature-dependent ¹H NMR spectra in C₂D₂Cl₄ solution were recorded and are shown in Figure 5. The first single peak assigned to the protons (Ha) of the bay position of TBC core shifted downfield by approximately $\Delta\delta = 0.18$ ppm when the temperature increased from 27 to 80 °C. The ¹H NMR spectrum of **TBC-C8** was featureless at 27 °C, and upon increasing the temperature to 50, 70, and 80 °C, all the resonances at the

aromatic region were shifted downfield and became distinct and sharp. This further supported that these new molecules, although they are nonplanar (vide infra), have a high tendency to aggregate in solution presumably via π - π interactions.

The solution of **TBC-C8** was drop-casted onto a Si wafer and the solvent was slowly evaporated under a saturated solvent atmosphere and the film was studied by SEM technique. Interestingly, uniform fibrous microstructures hundreds of nanometers in width and tens of micrometers in length were observed (Figure 6a,b). This unusual long-scale formation of regular microstructure from **TBC-C8** further indicates that there are strong intermolecular interactions in the newly designed tetrabenzocoronene derivatives. The well-defined self-assembled structures also open the opportunities to fabricate electronic devices on the individual fibers in future work. The saturated solutions of **TBC-C8** in

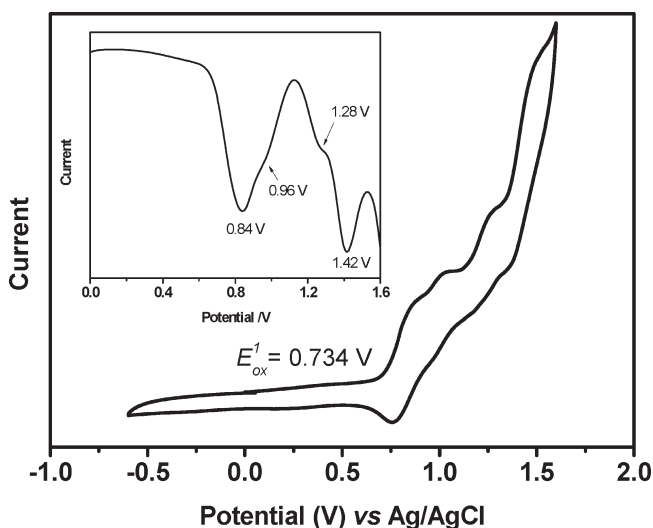


FIGURE 4. Cyclic voltammogram of **TBC-C8** in DCM with 0.1 M Bu₄NPF₆ as supporting electrolyte, AgCl/Ag as reference electrode, Au disk as working electrode, Pt wire as counter electrode, and scan rate at 50 mV/s. Insert: The differential pulse voltammogram.

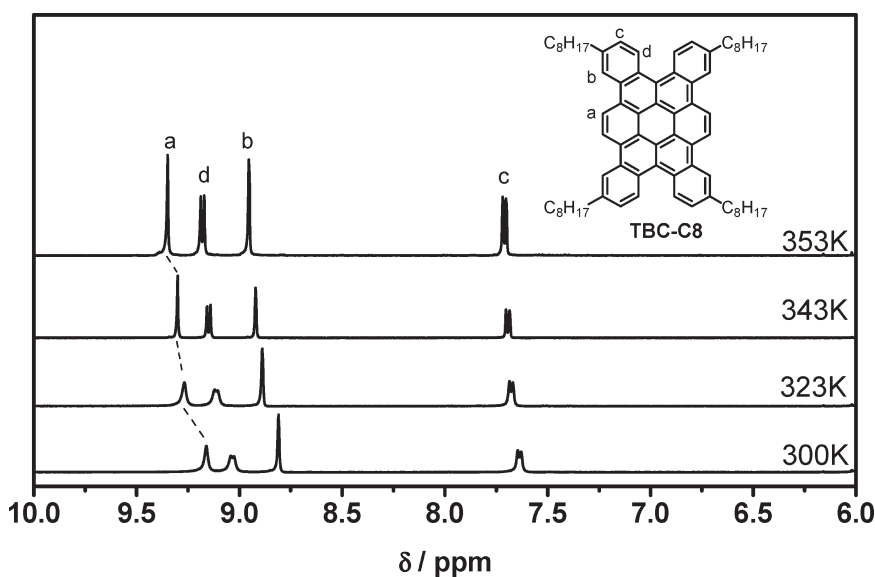


FIGURE 5. Aromatic region of the ¹H NMR spectra of compound **TBC-C8** in C₂D₂Cl₄ with concentration of 4 mg mL⁻¹ at different temperatures: 300, 323, 343, and 353 K. Insert: The molecular structure with respective peak assignments.

hexane and in toluene were aged for 3 days before dropping onto a 300 mesh copper TEM grid and the representative TEM images are shown in Figure 6, panels c and d. Rod-like structures were observed when the sample was prepared from hexane but large-area curved sheet-like structures were found when the solution was prepared from toluene. This indicated that the **TBC-C8** molecules self-organized into ordered structures in solution by intermolecular interactions.

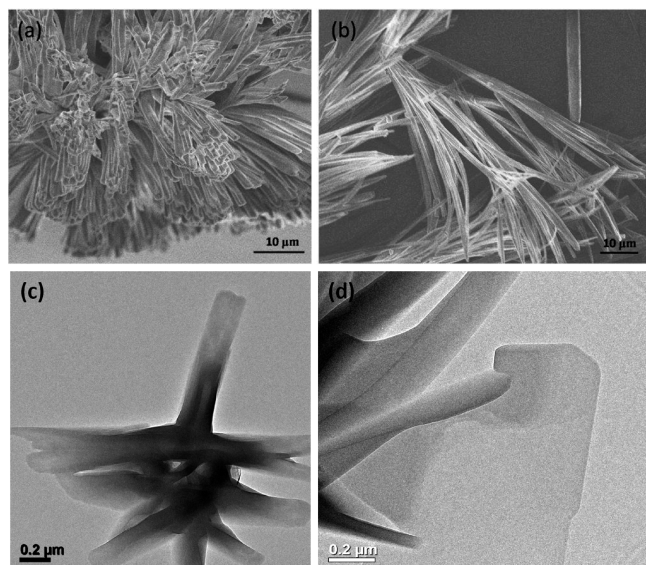


FIGURE 6. (a, b) SEM images of the thin films of **TBC-C8** prepared by drop-casting a hexane solution onto a Si substrate followed by slow evaporation of solvent. (c) TEM image recorded after deposition of a saturated solution of **TBC-C8** in hexane onto the TEM grid. (d) TEM image recorded after deposition of a saturated solution of **TBC-C8** in toluene onto the TEM grid.

Single-Crystal Structure, Thermal Behavior, and Self-Assembly of **TBC-C8 in the Solid State.** TGA was used to evaluate the thermal stability of **TBC-C8** and it demonstrated an onset of decomposition temperature at 360 °C under nitrogen atmosphere (see the Supporting Information). DSC measurement of **TBC-C8** showed a melting point at 106 °C and did not show any other mesophase transitions (see the Supporting Information). Slow cooling of the sample from melt resulted in growth of needle-like crystals as observed by polarizing optical microscopy (see the Supporting Information).

Single-crystal growth of **TBC-C8** was attempted by using different solvent systems and two types of crystals were obtained by slow diffusion of hexane to the chloroform solution. It turned out that only the rectangular shaped crystals are suitable for crystallographic analysis and the major needle-like crystals are actually polycrystalline materials. The single-crystal structure of **TBC-C8** in the rectangular shaped crystal is presented in Figure 7. As expected, due to steric overcrowding the framework of the molecule is bent and both of the two outer benzenoid rings in the right side (Figure 7a) point in the opposite direction than the two outer benzenoid rings at the left side, i.e., the whole molecule has a C_{2v} symmetry. The bending of the core is visualized most clearly in Figure 7c. Interestingly, the solid packing structure in this crystal form discloses that there are actually no π - π interactions between the rigid π -system and there is only close contact between the aliphatic chains and the π -surface via weak $[C-H \cdots \pi]$ interaction. This packing mode seems in contrast to the aggregation behavior of the **TBC-C8** in solution. It is worth noting that the molecule **TBC-C8** could also have another conformational stereoisomer with D_{2h} symmetry, i.e., with the right-up and left-down benzenoid rings bent in the same direction whereas the other two outer benzenoid rings are bent in the opposite direction. This conformation likely exists in the second crystal

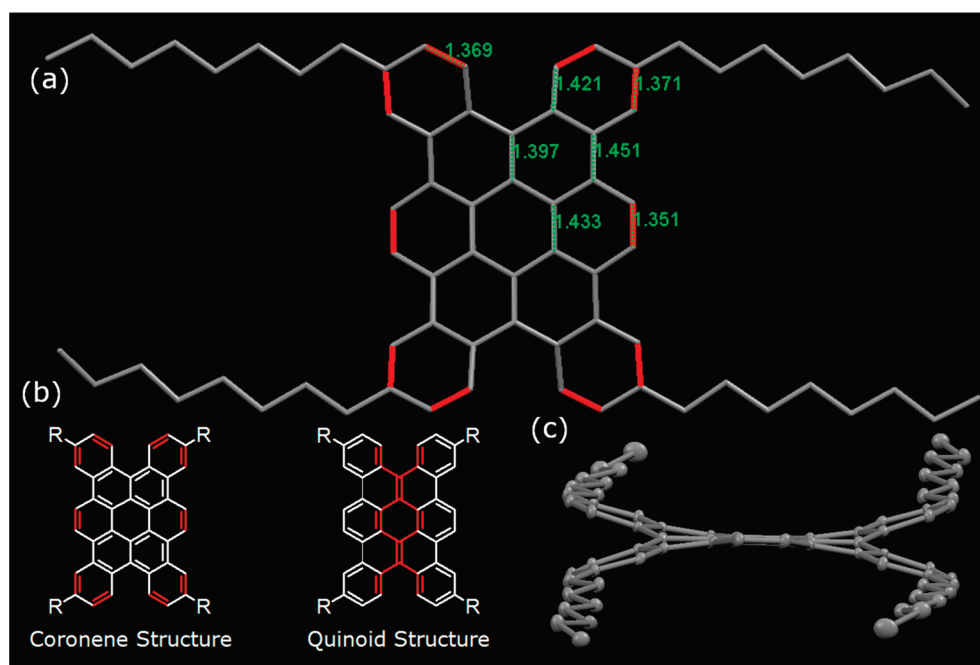


FIGURE 7. Single-crystal structure of **TBC-C8** grown from the $CHCl_3$ /hexane system (only the rectangular shaped crystals were analyzed). Hydrogen atoms have been removed for clarity. (a) Face-on view with marked bond length and (b) top view.

form but unfortunately we are not able to perform crystallographic analysis on these needle-like crystals, which is the major crystal formed. Intermolecular π - π interactions likely happen for this isomer. The wide-angle X-ray diffraction pattern of the polycrystalline powder of **TBC-C8** (see Figure S3 in the Supporting Information) disclosed an intense reflection peak at $d = 3.60$ Å, which can be correlated to the long-range ordered π - π stacking distance in a self-assembled columnar structure.

A comparison was also made between some of the bond lengths in this contorted tetrabenzocoronene derivative and those from the aromatic benzene ring and linear polyenes. One rising question is whether the TBC core tends to exist in a quinoid form in which the molecule can be drawn as six aromatic sextet rings together with a delocalized quinoid structure along the central axis (Figure 7b). The data clearly show that the bond length for the assumed quinoidal carbon-carbon double bond is 1.397 Å, which is much longer than that of isolated C=C bond (1.35 Å) but close to a delocalized carbon-carbon bond in benzene (1.38–1.40 Å). Thus the answer for this question is no. In fact, a short C=C bond (labeled in red) with bond length of 1.351 Å was observed for the nonfused benzenoid rings of the coronene core in **TBC-C8**, indicating that the tetrabenzocoronene actually has a similar electronic structure to the original coronene molecule.

Space-Charge Limited-Current (SCLC) Mobility Measurements. The charge carrier mobility of **TBC-C8** was determined by using the space-charge limited-current (SCLC) technique. The SCLC measurements were made in a cross-junction ITO/PEDOT:PSS/**TBC-C8**/Au cell (ITO: indium tin oxide), with a thick film of **TBC-C8** sandwiched between two electrodes. The thin film was made by drop-casting from 15 mg/mL chlorobenzene solution, and the average active layer film thickness was measured on an AMBIOS XP-1 high-resolution surface profiler. The Au electrode was prepared by thermally evaporating a 100-nm-thick Au layer with a mask shadow under vacuum at 10^{-4} Pa. The current-voltage characteristics were measured in a glovebox at room temperature (Keithley, Model 4200). In a typical experiment, the thickness of the **TBC-C8** is 1.6 μm . Current-voltage measurements (Figure 8) exhibit a typical linear region at low voltages, where the behavior is ohmic, and a quadratic region at higher voltages, where the current becomes space-charge-limited. Therefore, the SCLC mobility can be calculated from

$$J = \frac{9}{8} \frac{\epsilon_0 \epsilon_r \mu V^2}{d^3}$$

where J is the measured current density, μ the charge mobility, ϵ_0 the permittivity of free space, ϵ_r the dielectric constant of the material (a value of $\epsilon_r = 3$ is assumed here), V the applied voltage, and d the thickness of the device. The average SCLC mobility was obtained to be $0.61 \text{ cm}^2 \text{ V}^{-1} \text{ s}^{-1}$ for **TBC-C8**. This value is much higher than those for most other disk-like materials, likely due to the strong intermolecular interactions in **TBC-C8**.

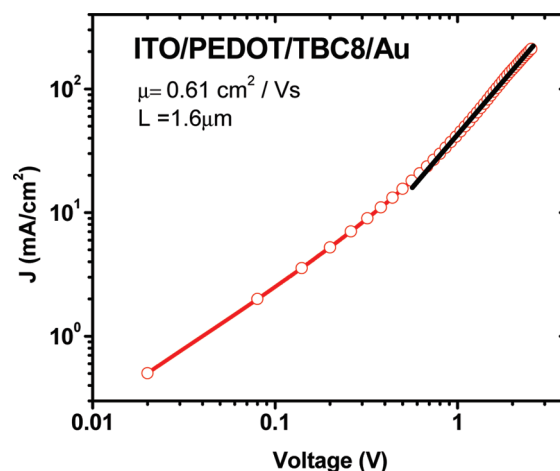


FIGURE 8. Double logarithmic plot of the current density (J) versus applied voltage (V) measured in a 1.6- μm -thick sample of **TBC-C8** at room temperature. Symbols represent experimental data and the continuous lines represent ideal quadratic regimes of the current, as a function of the applied voltage.

Conclusions

In summary, we have developed a new type of enlarged π -conjugated system based on the tetrabenzocoronene core that can be facilely prepared by two-step cyclodehydrogenation reactions from the substituted olefin precursors. Extended π -conjugation with desirable HOMO energy levels suitable for charge injection from electrodes was observed for the new material. Long-range columnar π -stacking was observed in the solid state although they are nonplanar contorted molecules. High SCLC charge carrier mobilities, with an average value of $0.61 \text{ cm}^2 \text{ V}^{-1} \text{ s}^{-1}$, were obtained for **TBC-C8**. The facile synthesis, the intriguing electronic property, the ordered self-assembly, and the high SCLC mobilities of this new type of materials qualify them as potential electrode-friendly hole-transporting semiconductors for electronic devices, such as field-effect transistors, light-emitting diodes, and solar cells.

Experimental Section

General. All reactions were carried out under an inert nitrogen atmosphere. Anhydrous tetrahydrofuran, benzene, and toluene were distilled over sodium under a nitrogen atmosphere. Photocyclization reaction was carried out in a photochemical reactor with irradiation of a 450 W medium pressure mercury vapor lamp. Column chromatography was performed on silica gel. All NMR spectra were recorded in solution and the chemical shifts are quoted in ppm, relative to tetramethylsilane, using the residual solvent peak as a reference standard. The melting point was measured without calibration. Low-resolution mass spectra were recorded with EI ionization source. High-resolution mass spectra were recorded with FAB ionization source. Elemental analyses were performed for C and H only. Solutions for the UV-vis absorption and fluorescence spectroscopic measurements were prepared in HPLC pure solvents. Cyclic voltammetry was performed on an electrochemical analyzer with a three-electrode cell in a solution of 0.1 M tetrabutylammonium hexafluorophosphate (Bu_4NPF_6) dissolved in dry DCM. The measurements for 1 mM compound **TBC-C8** were conducted at room temperature under nitrogen atmosphere at a scan rate of 50 mV s^{-1} . A gold disk, a Pt wire, and a Ag/AgCl electrode were used as the working electrode, counter electrode,

(18) Chi, C.; Wegner, G. *Macromol. Rapid Commun.* **2005**, *26*, 1532–1537.

(19) Talarico, M.; Termine, R.; Garcia-Frutos, E. M.; Omenat, A.; Serranoc, J.-L.; Gómez-Lor, B.; Golemme, A. *Chem. Mater.* **2008**, *20*, 6589–6591.

and reference electrode, respectively. The potential was calibrated against the ferrocene/ferrocenium couple. TGA was carried out at a heating rate of 10 deg min⁻¹ under nitrogen flow. DSC was performed at a heating/cooling rate of 10 deg min⁻¹ under nitrogen flow. The crystallographic data collection was carried out at 293 K. Powder X-ray diffraction measurement was performed at room temperature. SEM measurements were carried out on a field emission scanning electron microanalyzer at 5 kV. The samples for SEM were prepared by dropping a drop of dilute toluene solution of the **TBC-C8** onto a Si wafer and the solvent was allowed to evaporate slowly in a saturated toluene atmosphere at room temperature. TEM measurements were conducted at 200 keV. The saturated solutions of **TBC-C8** in hexane and toluene were aged for 3 days at room temperature and then dropped onto 300 mesh copper TEM grids.

Synthesis of Thioketone 2a. Benzophenone (**1a**, 2.73 g, 15.0 mmol) and Lawesson's reagent (0.6 eq, 3.60 g, 9.0 mmol) were added to 120 mL of toluene. The solution was heated to 80 °C under nitrogen atmosphere for 12 h. The dark blue solution was allowed to cool to room temperature and 200 mL of a mixture solvent of hexane and DCM (4:1, v/v) was added. The mixture was filtrated through a plug of silica gel and washed with a small amount of the same eluent. The solvent of the filtrate was removed under vacuum and the crude product **2a** was isolated as a blue solid (2.90 g). Compound **2a** is not stable so the crude product was used for the next step immediately. ¹H NMR (300 MHz, CDCl₃, 300 K, ppm) δ 7.81 (d, *J* = 6.96 Hz, 4H), 7.59 (t, *J* = 7.65 Hz, 4H), 7.49 (t, *J* = 7.68 Hz, 2H). It is hard to obtain ¹³C NMR spectra and MS spectra due to the poor stability of **2a**.

Synthesis of Thioepoxide 3a. A 1.2 equiv sample of 10-diazoanthrone¹⁶ (3.30 g, 15.0 mmol) dissolved in THF (50 mL) was added dropwise to a solution of thioketone **2a** (2.55 g, 14.0 mmol) in THF (150 mL). After addition, the reaction was stirred for 15 h. After removal of solvent under vacuum, the residue was purified by column chromatography (silica gel, 4:1 hexane:DCM, *R_f* = 0.3) to give compound **3a** as a white solid (3.34 g, 57%), mp 230.2–231.5 °C. ¹H NMR (500 MHz, CDCl₃, 300 K, ppm) δ 8.28 (d, *J* = 7.55 Hz, 2H), 7.32 (t, *J* = 7.60 Hz, 2H), 7.25 (d, *J* = 8.20 Hz, 2H), 7.10 (m, 6H), 6.95 (m, 6H). ¹³C NMR (125 MHz, CDCl₃, 300 K, ppm) δ 184.8, 141.6, 139.8, 134.3, 131.9, 129.2, 128.9, 127.8, 127.6, 127.0, 126.7, 70.5, 56.6. MS (EI) calcd for C₂₇H₁₈OS (M+) 390.11, found 390.10. Anal. Calcd for C₂₇H₁₈OS: C, 83.05; H, 4.65. Found: C, 83.31; H, 4.52.

Synthesis of Ketone 4a. A solution of the thioepoxide **3a** (3.00 g, 7.68 mmol) and triphenylphosphine (2.40 g, 9.20 mmol) in anhydrous toluene (120 mL) was heated at reflux under nitrogen atmosphere for 24 h. After being cooled to room temperature, the solvent was removed under reduced pressure. The solid residue was purified by column chromatography (silica gel, 3:1 hexane: DCM, *R_f* = 0.4) and ketone **4a** was isolated as a light yellow solid (2.60 g, 95%), mp 216.0–216.8 °C. ¹H NMR (500 MHz, CDCl₃, 300 K, ppm) δ 8.20 (d, *J* = 7.55 Hz, 2H), 7.30 (m, 12H), 7.19 (d, *J* = 8.20 Hz, 2H), 7.12 (t, *J* = 7.55 Hz, 2H). ¹³C NMR (125 MHz, CDCl₃, 300 K, ppm) δ 186.0, 146.2, 143.0, 139.4, 133.0, 130.7, 130.5, 129.2, 129.1, 128.6, 127.2, 127.1, 126.4. MS (EI) calcd for C₂₇H₁₈O (M+) 358.14, found 358.20. Anal. Calcd for C₂₇H₁₈O: C, 90.47; H, 5.06. Found: C, 90.22; H, 5.03.

Synthesis of Thioketone 5a. The procedure for the synthesis of **2a** was followed to prepare **5a** from **4a** and Lawesson's reagent. Compound **5a** was obtained as a dark green solid in 91% yield. ¹H NMR (300 MHz, CDCl₃, 300 K, ppm) δ 8.34 (d, *J* = 7.38 Hz, 2H), 7.23 (m, 12H), 7.10 (m, 4H). It is hard to obtain ¹³C NMR spectra and MS spectra due to the poor stability of **5a**.

Synthesis of Thioepoxide 6a. A 1.1 equiv sample of diphenyldiazomethane^{12a} dissolved in 20 mL of DCM was added dropwise to a solution of thioketone **5a** (1.12 g, 3.00 mmol) in

THF (50 mL). After addition, the reaction was stirred for 15 h. After removal of solvents under vacuum, the residue was purified by column chromatography (silica gel, 2:1 hexane: DCM, *R_f* = 0.3) to give compound **6a** as a white solid (1.00 g, 89%), mp 254.3–255.5 °C. ¹H NMR (500 MHz, CDCl₃, 300 K, ppm) δ 7.47 (d, *J* = 7.55 Hz, 4H), 7.42 (d, *J* = 8.20 Hz, 2H), 7.38 (d, *J* = 6.95 Hz, 4H), 7.25 (m, 6H), 7.16 (d, *J* = 6.95 Hz, 2H), 7.10 (m, 6H), 6.86 (t, *J* = 7.55 Hz, 2H), 6.77 (t, *J* = 7.60 Hz, 2H). ¹³C NMR (125 MHz, CDCl₃, 300 K, ppm) δ 142.2, 140.7, 139.9, 138.9, 136.3, 133.8, 130.4, 130.0, 128.5, 128.3, 128.0, 127.3, 126.8, 126.0, 125.8, 69.6, 63.7. MS (EI) calcd for C₄₀H₂₈S (M+) 540.19, found 540.20. Anal. Calcd for C₄₀H₂₈S: C, 88.85; H, 5.22. Found: C, 88.52; H, 5.60.

Synthesis of 7a. The procedure for the synthesis of **4a** was followed to prepare **7a** from **6a** and triphenylphosphine. Compound **7a** was obtained as a white solid in 87% yield, mp 309.4–310.0 °C. ¹H NMR (500 MHz, CDCl₃, 300 K, ppm) δ 7.43 (d, *J* = 8.20 Hz, 8H), 7.30 (t, *J* = 7.55 Hz, 8H), 7.22 (t, *J* = 7.55 Hz, 4H), 7.00 (m, 4H), 6.73 (m, 4H). ¹³C NMR (125 MHz, CDCl₃, 300 K, ppm) δ 142.5, 139.8, 137.8, 135.6, 129.7, 128.2, 127.9, 126.6, 125.1. MS (EI) calcd for C₄₀H₂₈ (M+) 508.22, found 508.30. Anal. Calcd for C₄₀H₂₈: C, 94.45; H, 5.55. Found: C, 94.10; H, 5.66.

Synthesis of 8a. The photolysis setup has been previously described.¹⁷ A mixture of compound **7a** (508 mg, 1.00 mmol), iodine (1.28 g, 5.00 mmol), and propylene oxide (20 mL) in anhydrous benzene (250 mL) was irradiated with a 450 W medium-pressure mercury vapor lamp in an immersion well, under argon atmosphere. After 16 h of irradiation, the solvent was removed under reduced pressure and a yellow powder precipitate was collected. Compound **8a** (389 mg, 77%) was isolated by column chromatography (4:1 chloroform:THF, *R_f* = 0.6), mp 348.0–349.1 °C. ¹H NMR (500 MHz, CDCl₃, 300 K, ppm) δ 9.14 (s, 2H), 9.00 (d, *J* = 8.20 Hz, 2H), 8.03 (d, *J* = 8.20 Hz, 2H), 7.76 (t, *J* = 6.95 Hz, 2H), 7.60 (m, 10H), 7.50 (m, 4H), 6.76 (m, 2H). ¹³C NMR (125 MHz, CDCl₃, 300 K, ppm) δ 141.7, 134.6, 133.6, 132.4, 131.9, 130.6, 129.5, 129.0, 127.8, 127.6, 127.4, 126.9, 126.5, 126.2, 125.7, 125.4, 122.8, 121.7. MS (EI) calcd for C₄₀H₂₄ (M+) 504.19, found 504.30. Anal. Calcd. for C₄₀H₂₄: C, 95.21; H, 4.79. Found: C, 94.84; H, 5.08.

Synthesis of TBC. Compound **8a** (100 mg, 0.20 mmol) was dissolved in dichloromethane (60 mL) in a 250-mL two-necked round-bottomed flask. A constant stream of argon was bubbled into the solution through a glass capillary. A solution of FeCl₃ (0.74 g, 4.60 mmol) in CH₃NO₂ (10 mL) was then added dropwise via syringe. Throughout the whole reaction, a constant stream of argon was bubbled through the mixture to remove HCl formed in situ. The reaction was stirred for 25 min and then quenched by adding methanol (200 mL). The precipitate was collected by filtration, washed with methanol, hexane, and chloroform, and dried under vacuum to afford **TBC** as a yellow solid (56 mg, 57% yield), mp > 400 °C. It is hard to record ¹H NMR and ¹³C NMR spectra due to the poor solubility and strong π -stacking of **2a**. MS (EI) calcd for C₄₀H₂₀ (M+) 500.16, found 500.30. HRMS (FAB+) calcd for C₄₀H₂₀ 500.1565, found 500.1572 (error = 1.4 ppm). Anal. Calcd. for C₄₀H₂₀: C, 95.97; H, 4.03. Found: C, 95.81; H, 3.97.

Synthesis of TBC-C8. **Synthesis of Thioketone 2b** The procedure for the synthesis of **2a** was followed to prepare **2b** from 4,4'-dioctylbenzophenone (**1b**, see the synthesis in the Supporting Information) and Lawesson's reagent. Compound **2b** was obtained as a dark blue oil in 95% yield. ¹H NMR (300 MHz, CDCl₃, 300 K, ppm) δ 7.65 (d, *J* = 8.40 Hz, 4H), 7.18 (d, *J* = 8.37 Hz, 4H), 2.65 (t, *J* = 7.56 Hz, 4H), 1.63 (m, 4H), 1.30 (m, 20H), 0.89 (m, 6H). ¹³C NMR (75 MHz, CDCl₃, 300 K, ppm) δ 147.8, 145.3, 129.9, 128.0, 36.0, 31.9, 31.0, 29.4, 29.3, 29.2, 22.6, 14.0. MS (EI) calcd for C₂₉H₄₂S (M+) 422.30, found 422.40.

Synthesis of Thioepoxide 3b. The procedure for the synthesis of **3a** was followed to prepare **3b**. Compound **3b** was obtained as

a translucent oil in 76% yield. $^1\text{H NMR}$ (500 MHz, CDCl_3 , 300 K, ppm) δ 8.27 (d, $J=7.55$ Hz, 2H), 7.30 (t, $J=7.55$ Hz, 2H), 7.23 (d, $J=7.55$ Hz, 2H), 7.07 (t, $J=7.60$ Hz, 2H), 6.93 (d, $J=8.20$ Hz, 4H), 6.74 (d, $J=7.60$ Hz, 4H), 2.37 (m, 4H), 1.42 (m, 4H), 1.23 (m, 20H), 0.88 (m, 6H). $^{13}\text{C NMR}$ (125 MHz, CDCl_3 , 300 K, ppm) δ = 184.9, 141.3, 140.1, 139.0, 134.3, 131.8, 129.03, 129.00, 127.62, 127.59, 126.9, 70.5, 56.8, 35.2, 31.9, 31.2, 29.4, 29.3, 29.0, 22.7, 14.1. MS (EI) calcd for $\text{C}_{43}\text{H}_{50}\text{OS}$ (M^+) 614.36, found 614.50. HRMS (FAB+) calcd for $\text{C}_{43}\text{H}_{50}\text{OS}$ 614.3582, found 614.3570 (error = -1.9 ppm).

Synthesis of Ketone 4b. The procedure for the synthesis of **4a** was followed to prepare **4b** from **3b** and triphenylphosphine. Compound **4b** was obtained as a red oil in 94% yield. $^1\text{H NMR}$ (300 MHz, CDCl_3 , 300 K, ppm) δ 8.15 (d, $J=7.89$ Hz, 2H), 7.28 (m, 2H), 7.08 (m, 12H), 2.55 (t, $J=7.41$ Hz, 4H), 1.59 (m, 4H), 1.28 (m, 20H), 0.86 (m, 6H). $^{13}\text{C NMR}$ (75 MHz, CDCl_3 , 300 K, ppm) δ 186.1, 146.8, 141.9, 140.4, 139.7, 132.9, 130.3, 130.2, 129.2, 129.0, 128.5, 127.0, 126.3, 35.6, 31.9, 31.2, 29.4, 29.3, 29.2, 22.6, 14.1. MS (EI) calcd for $\text{C}_{43}\text{H}_{50}\text{O}$ (M^+) 582.39, found 582.50. HRMS (FAB+) calcd for $\text{C}_{43}\text{H}_{50}\text{O}$ 582.3862, found 582.3878 (error = 2.8 ppm).

Synthesis of Thioketone 5b. The procedure for the synthesis of **5a** was followed to prepare **5b** from **4b** and Lawesson's reagent. Compound **5b** was obtained as a dark green oil in 90% yield. $^1\text{H NMR}$ (500 MHz, CDCl_3 , 300 K, ppm) δ 8.35 (d, $J=6.95$ Hz, 2H), 7.21 (t, $J=8.20$ Hz, 2H), 7.08 (m, 12H), 2.55 (t, $J=7.55$ Hz, 4H), 1.55 (m, 4H), 1.28 (m, 20H), 0.89 (m, 6H). $^{13}\text{C NMR}$ (125 MHz, CDCl_3 , 300 K, ppm) δ 223.0, 146.8, 141.9, 141.1, 140.3, 133.4, 131.8, 129.9, 129.0, 128.5, 127.7, 126.9, 35.6, 31.8, 31.2, 29.4, 29.3, 29.2, 22.6, 14.1. MS (EI) calcd for $\text{C}_{43}\text{H}_{50}\text{S}$ (M^+) 598.36, found 598.50.

Synthesis of Thioepoxide 6b. The procedure for the synthesis of **6a** was followed to prepare **6b**. Compound **6b** was obtained as a translucent oil in 82% yield. $^1\text{H NMR}$ (500 MHz, CDCl_3 , 300 K, ppm) δ 7.41 (d, $J=7.60$ Hz, 2H), 7.33 (d, $J=6.95$ Hz, 4H), 7.25 (d, $J=8.20$ Hz, 4H), 7.12 (d, $J=7.60$ Hz, 2H), 7.04 (d, $J=7.60$ Hz, 4H), 6.88 (d, $J=7.55$ Hz, 4H), 6.83 (t, $J=7.55$ Hz, 2H), 6.74 (t, $J=7.55$ Hz, 2H), 2.58 (m, 4H), 2.48 (m, 4H), 1.61 (m, 4H), 1.54 (m, 4H), 1.30 (m, 40H), 0.88 (m, 12H). $^{13}\text{C NMR}$ (75 MHz, CDCl_3 , 300 K, ppm) δ 141.3, 141.2, 139.8, 139.5, 139.2, 138.3, 136.5, 133.4, 130.3, 129.9, 128.5, 128.3, 127.8, 127.2, 125.7, 125.5, 69.6, 64.0, 35.6, 35.4, 31.9, 31.3, 31.2, 29.5, 29.34, 29.30, 29.26, 22.7, 14.1. MS (EI) calcd for $\text{C}_{72}\text{H}_{92}\text{S}$ (M^+) 988.69, found 989.80. HRMS (FAB+) calcd for $\text{C}_{72}\text{H}_{92}\text{S}$ 988.6920, found 988.6889 (error = -3.1 ppm).

Synthesis of Olefin 7b. The procedure for the synthesis of **7a** was followed to prepare **7b** from **6b** and triphenylphosphine.

Compound **7b** was obtained as a white solid in 97% yield, mp 90.0–91.0 °C. $^1\text{H NMR}$ (300 MHz, CDCl_3 , 300 K, ppm) δ 7.29 (d, $J=8.07$ Hz, 8H), 7.07 (d, $J=8.04$ Hz, 8H), 6.96 (m, 4H), 6.68 (m, 4H), 2.56 (t, $J=7.38$ Hz, 8H), 1.61 (m, 8H), 1.28 (m, 40H), 0.88 (m, 12H). $^{13}\text{C NMR}$ (75 MHz, CDCl_3 , 300 K, ppm) δ 141.1, 139.9, 139.7, 138.0, 135.2, 129.5, 128.1, 127.9, 124.8, 35.6, 31.9, 31.3, 29.5, 29.4, 29.3, 22.7, 14.1. MS (EI) calcd for $\text{C}_{72}\text{H}_{92}$ (M^+) 956.72, found 957.00. HRMS (FAB+) calcd for $\text{C}_{72}\text{H}_{92}$ 956.7199, found 956.7216 (error = 1.8 ppm).

Synthesis of 8b. The procedure for the synthesis of **8a** was followed to prepare **8b**. Compound **8b** was obtained as a light yellow oil in 71% yield. $^1\text{H NMR}$ (300 MHz, CDCl_3 , 300 K, ppm) δ 9.13 (s, 2H), 8.79 (s, 2H), 8.01 (d, $J=8.55$ Hz, 2H), 7.50 (m, 8H), 7.38 (d, $J=8.04$ Hz, 4H), 6.75 (m, 2H), 2.98 (t, $J=7.38$ Hz, 4H), 2.78 (t, $J=7.41$ Hz, 4H), 1.80 (m, 8H), 1.40 (m, 40H), 0.92 (m, 12H). $^{13}\text{C NMR}$ (75 MHz, CDCl_3 , 300 K, ppm) δ 142.0, 140.8, 139.1, 134.5, 133.7, 132.2, 130.5, 130.3, 129.6, 129.0, 127.6, 127.5, 127.1, 126.5, 126.0, 124.9, 121.8, 121.4, 36.5, 35.8, 31.9, 31.7, 31.5, 29.6, 29.6, 29.5, 29.34, 29.32, 29.30, 22.71, 22.70, 14.1. MS (EI) calcd for $\text{C}_{72}\text{H}_{88}$ (M^+) 952.69, found 953.00. HRMS (FAB+) calcd for $\text{C}_{72}\text{H}_{88}$ 952.6886, found 952.6906 (error = 2.1 ppm).

Synthesis of TBC-C8. The procedure for the synthesis of **TBC** was followed to prepare **TBC-C8**. Compound **TBC-C8** was obtained as a light yellow solid in 92% yield, mp 106 °C (by DSC). $^1\text{H NMR}$ (500 MHz, CDCl_3 , 343 K, ppm) δ 9.30 (s, 4H), 9.15 (d, $J=8.85$ Hz, 4H), 8.92 (s, 4H), 7.69 (d, $J=8.85$ Hz, 4H), 3.11 (t, $J=7.55$ Hz, 8H), 2.02 (m, 8H), 1.62 (m, 8H), 1.54 (m, 8H), 1.40 (m, 24H), 0.97 (m, 12H). $^{13}\text{C NMR}$ (125 MHz, CDCl_3 , 300 K, ppm) δ 141.0, 130.1, 129.3, 127.0, 126.63, 126.57, 124.2, 123.5, 122.3, 121.8, 121.3, 36.3, 31.6, 31.2, 29.4, 29.3, 29.0, 22.4, 13.7. MS (EI) calcd for $\text{C}_{72}\text{H}_{84}$ (M^+) 948.66, found 948.80. HRMS (FAB+) calcd for $\text{C}_{72}\text{H}_{84}$ 948.6568, found 948.6582 (error = 1.5 ppm).

Acknowledgment. This work was financially supported by the Singapore NRF Competitive Research Program (R-143-000-360-281) and NUS Young Investigator Award (R-143-000-356-101).

Supporting Information Available: Experimental procedures of some intermediates, characterization data of all new compounds, TGA and DSC spectrum, powder X-ray diffraction data, and X-ray crystallographic analysis data. This material is available free of charge via the Internet at <http://pubs.acs.org>.